ELSEVIER

European Journal of Pharmacology 414 (2001) 177–188

ejp

www.elsevier.nl/locate/ejphar

Oxidative stress and c-Jun-amino-terminal kinase activation involved in apoptosis of primary astrocytes induced by disulfiram–Cu^{2+} complex

Sung Ho Chen [a], Shing Hwa Liu [a], Yu-Chih Liang [b], Jen-Kun Lin [b], Shoei-Yn Lin-Shiau [a,c,*]

[a] *Institute of Toxicology, College of Medicine, National Taiwan University, Taipei, Taiwan*
[b] *Institute of Biochemistry, College of Medicine, National Taiwan University, Taipei, Taiwan*
[c] *Institute of Pharmacology, College of Medicine, National Taiwan University, Taipei, Taiwan*

Received 4 September 2000; received in revised form 23 January 2001; accepted 26 January 2001

Abstract

Disulfiram is frequently used in the treatment of alcoholism. In this study, we found that $CuCl_2$ (1–10 μM), but not other metal ions (Fe^{2+}, Zn^{2+}, Pb^{2+}), markedly potentiated disulfiram-induced cytotoxicity by 440-fold in primary astrocytes. Thus, the molecular mechanisms of the cytotoxic effects induced by the disulfiram–Cu^{2+} complex were explored. The changes in morphology (nuclear condensation and apoptotic body formation) and hypodiploidy of DNA suggested that the disulfiram–Cu^{2+} complex induced an apoptotic process. Our studies of the death-signaling pathway reveal that decreased mitochondrial membrane potential, increased free radical production, and depletion of non-protein-thiols (glutathione) were involved. The disulfiram–Cu^{2+} complex activated c-Jun-amino-terminal kinase (JNK) and caspase-3 followed by poly (ADP-ribose) polymerase degradation in a time-dependent manner. Moreover, the cellular Cu content was markedly increased and the copper chelator bathocuproine disulfonate abolished all of these cellular events, suggesting that Cu^{2+} is essential for death signaling. The antioxidants *N*-acetylcysteine and vitamin C also inhibited the cytotoxic effect. Thus, we conclude that the disulfiram–Cu^{2+} complex induces apoptosis and perhaps necrosis at a late stage mediated by oxidative stress followed by sequential activation of JNK, caspase-3 and poly (ADP-ribose) polymerase degradation. These findings imply that the axonal degeneration and neurotoxicity observed after the chronic administration of disulfiram are perhaps, at least in part, due to the cytotoxic effect of the disulfiram–Cu^{2+} complex formed endogenously. © 2001 Published by Elsevier Science B.V.

Keywords: Disulfiram; Oxidative stress; Membrane potential; Bathocuproine disulfonate; c-Jun-amino-terminal kinase (JNK); Caspase-3

1. Introduction

Disulfiram is an inhibitor of aldehyde dehydrogenase and clinically used in the treatment of alcoholism (under the trade name Antabus or Aversan) (Johansson, 1992). The nauseating effect of acetaldehyde deters the continued consumption of ethanol (Goedde and Agarwal, 1992). It has been reported that chronic administration of disulfiram causes axonal degeneration (Ansbacher et al., 1982). Other in vivo reports point out that disulfiram causes oxidative stress (Delmaestro and Trombetta, 1995), sister chromatid exchanges (Madrigal-Bujaidar et al., 1999), mitochondrial alterations (Simonian et al., 1992) and dopaminergic malfunctions (Vaccari et al., 1996). However, the molecular mechanisms of the toxic effects of disulfiram still remain to be elucidated. In this study, we used cultured rat cortical astrocytes as a model system for elucidating the possible molecular mechanisms of the cytotoxic effects of disulfiram.

Astrocytes, the major cell types in the brain (Kuffler et al., 1984), are important in protecting neurons from various external insults (Langeveld et al., 1995; Brown, 1999). They can secrete various neurotrophic factors (interleukin-6, glial-derived neurotrophic factor) to promote the growth of neurons. Moreover, they are a sink for excessive neurotoxic glutamate and modulate the extracellular K^+ concentrations, enabling neurons to function optimally. Thus, we performed this study with primary cultures of rat cortical

* Corresponding author. Institute of Toxicology, College of Medicine, National Taiwan University, Section 1, Jen-Ai Road, No. 1, Taipei, 10043, Taiwan. Tel.: +886-2-23123456; fax: +886-2-23410217.
E-mail address: syl@ha.mc.ntu.edu.tw (S.-Y. Lin-Shiau).

0014-2999/01/$ - see front matter
PII: S0014-2999(01)00792-0

astrocytes in order to understand the action mechanism of disulfiram.

During this study, we tested the effects of several essential metal ions (Cu^{2+}, Zn^{2+}, Fe^{2+}) on the cytotoxic effects of disulfiram. We found that only Cu^{2+} exerted a unique potentiating effect on disulfiram-induced cytotoxicity. Cu^{2+} is a metal ion essential for the activation of many enzymes such as Cu/Zn superoxide dismutase and dopamine β-hydroxylase (Kennedy et al., 1998; Talbot, 1986). The copper-carried protein-chaperon is abundant in astrocytes (Rothstein et al., 1999). In addition, copper compounds are also widely used in agricultural pesticides (Bezuglyi et al., 1982) and in industrial processes (Kostova, 1995). Thus, it is important to understand the mechanisms of the toxic effects of disulfiram–Cu^{2+} complex in cultured astrocytes. Our findings showed that low concentrations (< 1 μM) of disulfiram plus a low concentration (10 μM) of $CuCl_2$ markedly decreased mitochondrial membrane potential, increased free radical production and depleted the content of non-protein-thiols (glutathione). Subsequently, the disulfiram–Cu^{2+} complex activated c-Jun-terminal kinase (JNK), caspase-3 and poly (ADP-ribose) polymerase degradation, which was presumably responsible for inducing the apoptotic process in the cultured rat cortical astrocytes. These findings suggest the possibility that the neurotoxic effects of disulfiram can be, at least in part, due to a detrimental effect on astrocytes.

2. Materials and methods

2.1. Materials

Dulbecco's modified Eagle's medium (DMEM), fetal calf serum, and other cell culture supplements were obtained from FALCON. (3–4, 5-dimethyl thiazol-2-yl)-2,5-diphenyl tetrazolium bromide (MTT), $CuCl_2$, vitamin C, catalase, superoxide dismutase, glutathione, and *N*-acetylcysteine are water soluble and were purchased from Sigma (St. Louis, MO, USA). Disulfiram and bathocuproine disulfonate from Sigma, benzyloxycarbonyl-Asp-Glu-Val-Asp(Ome)-fluoromethyl ketone (Z-DEVD-FMK) (Calbiochem, La Jolla, California, USA), Höechst 33258, 3,3′-dihexyloxacarbocyanine iodide (DiOC6(3)) and 2′, 7′-dichlorofluorescein diacetate (DCFHDA) from molecular Probe (Eugene, OR, USA) are water insoluble and were dissolved in dimethyl sulfoxide (DMSO). [γ^{32}P] ATP was obtained from Amersham Life Science. Antibodies to JNK-1, extracellular signal regulated kinase 1 (ERK-1), p38, Bcl-2, and poly (ADP-ribose) polymerase were purchased from Santa Cruz (Santa Cruz, California, USA). The final concentration of DMSO in the incubation medium was less than 0.5% to prevent a toxic effect of DMSO. Water and the respective concentration of DMSO were used as a control vehicle.

2.2. Cell cultures

Astrocytes were prepared from 1-day-old Wistar rat pups (Tedeschi et al., 1986). In brief, cortices were isolated and cleaned of white matter and meninges, minced, and digested with trypsin (0.3 mg/ml) for 25 min. After that, we applied DNase (23.5 U/ml) to digest extracellular oligonucleotide, and trypsin inhibitor (0.3 mg/ml) to terminate the digestion of trypsin. The dissociated tissue was diluted with DMEM supplemented with 10% fetal bovine serum and seeded into cultured dishes or coverslips. The astrocytes on the cultured dishes were cultured to confluence (14 days) in a 5% CO_2 incubator at 37 ± 0.5°C. The culture medium was changed every 3–4 days. When the medium was changed, the culture dishes were gently shaken to remove the loosely adherent oligodendrocytes and microglia from the astrocyte monolayer, which were then decanted with the medium. Astrocyte cultures were characterized for purity as previously described (Amruthesh et al., 1993) and found to be 95% pure as assessed by the presence of glial fibrillary acidic protein (GFAP).

2.3. Cell viability assay

The cytotoxic effects of applied reagents were estimated after incubation with rat cortical astrocytes for various intervals using the MTT test (Denizot and Lang, 1986). The viability of rat cortical astrocytes was estimated by the ability to reduce the dye (3–4,5-dimethyl thiazol-2-yl)-2,5-diphenyl tetrazolium bromide (MTT) to blue purple formazan crystal. The products were dissolved in glycine buffer containing DMSO for quantification by measuring the optical density at 570 nm using an ELISA reader (Dynatech MR-7000).

2.4. Morphological features of astrocytes

After incubation with the applied reagents for various intervals, the rat cortical astrocytes were fixed with 4% paraformaldehyde. Photomicrographs were obtained with $40\times$ objective lens on a Zeiss Axiovert 135-TV microscope.

2.5. Höechst staining

Astrocytes were grown on coverslips. Cells were stimulated according to experimental protocols and then fixed with 4% paraformaldehyde for 30 min at room temperature. Samples were washed with phosphate-buffered saline (PBS) twice. The samples were incubated in 0.5% Triton X-100 for 10 min, stained with 3 μg/ml Höechts dye 33258 for 40 min, and washed with PBS. The nuclei were examined using an OLYMPUS IMT-2 fluorescence microscope (UV excitation and 475 nm emission) for apoptotic

bodies which were stained and emitted a green fluorescence.

2.6. Hypodiploid cell assay

Cells were collected, washed with ice-cold PBS, and then fixed in 70% ethanol at—20°C for at least 1 h. After fixation, the cells washed twice, incubated in 0.5 ml of 0.5% Triton X-100/PBS at 37 ± 0.5°C for 30 min with 1 mg/ml of RNase A, and stained with 0.5 ml of 50 μg/ml propidium iodide for 10 min. The fluorescence emitted from the propidium iodide–DNA complex was quantitated after laser excitation of the fluorescent dye by a FACScan flow cytometry (Becton Dickinson).

2.7. Determination of total intracellular Cu content

After treatment according to the experimental protocols, the astrocytes (6×10^6) were trysinized and centrifuged. The pellets were washed three times with 15 mM HEPES in 0.9% NaCl. (W/V), pH 7.3, and contamination with the external copper was minimized as described previously (Zhang et al., 1993). The different cellular fractions (membrane, cytosol and nuclei) were obtained by differential centrifugation and then extracted with different lysis buffers as described by Chen et al. (1995). An aliquot was removed for protein determination with a biocinchoninic acid (BCA) kit. The remainder was resuspended in 1.0 N nitric acid for analysis. The Cu standard was a commercially available solution of 1000 ppm (1000 mg/l) for atomic absorption spectrophotometry. This solution was diluted to various concentrations (10–200 ppb) with 0.1 N nitric acid. The Cu content of samples was analyzed by using a model Z-8200 atomic absorption spectrophotometer (Hitachi, Tokyo) with a graphite furnace (flameless mode).

In other experiments, the metal content of whole cells was measured by using an ICP-MS instrument (Friel et al., 1990). An aliquot of astrocytes was removed for protein assay and then the residue was resuspended in 0.1% Triton X-100/0.2% nitric acid for analysis. The commercial standard for trace metals (National Research Council Canada) was used and digested twice in Teflon cup in a high-pressure microwave acid-digestion bomb (Parr Instrument, Moline, IL, USA), before being analyzed by ICP-MS. The trace metal content was measured with the ICP-MS instruments (model Elan Model 250, Scuex, Thornhill, Ontario, Canada). The data were analyzed with Lotus 123 software (Lotus, Cambridge, MA, USA).

2.8. Measurement of mitocondrial membrane potential

Mitocondrial membrane potential was determined as the retention of the dye 3,3′-dihexyloxacarbocyanine, $DiOC_6(3)$ (Pastorino et al., 1998). After treatment, the cells were trypsinized and washed with PBS. Then the cells (1×10^6 cells in 500 μl PBS) were loaded with 50 nM $DiOC_6(3)$ and incubated at 37 ± 0.5°C for 15 min. The fluorescence intensity of $DiOC_6(3)$ was determined by FACScan flow cytometry (Becton Dickinson).

2.9. Measurements of non-protein thiols

The intercellular content of non-protein thiol groups (essentially contained in reduced glutathione) was determined by the method described by Griffith (1980). Briefly, the cells were trypsinized and washed with ice-cold PBS and then lysed with modified radioimmunoprecipitation assay (RIPA) buffer. An aliquot was removed to detect protein concentration, and the residue was treated with 5% trichloroacetic acid to precipitate the proteins. The proteins were discarded after centrifugation at $12{,}000 \times g$ for 10 min and the supernatant (50 μl) was reacted with 20 μl of 5,5-dithiobis-2-nitrobenzoic acid (DTNB, 1.2 mM) in 0.15 M imidazole buffer solution (pH 7.4). The non-protein thiol content was determined by a colorimetric assay at 412 nm with the respective glutathione standard.

2.10. Determination of free radical production

Free radical production was monitored with the fluorescent dye 2′,7′-dichlorofluorescin diacetate (DCFHDA) using a flow cytometric analyzer. Briefly, cells (1×10^6) were co-incubated with 30 μM DCFHDA in the presence of disulfiram–Cu^{2+} complex for various times at 37 ± 0.5°C. After incubation, the cells were carefully collected and fluorescence intensity was determined by flow cytometric analysis (Rosenkranz et al., 1992).

2.11. Caspase activity

Cells were trypsinized and washed with PBS. Then the cells were lysed with RIPA solution containing 25 mM HEPES (pH 7.5) buffer, 5 mM $MgCl_2$, 5 mM ethylenediaminetetra acetic acid (EDTA), 5 mM dithiothreitol, 2 mM phenylmethylsulfonyl fluoride, 10 μg/ml pepstatin A and 10 μg/ml leupeptin, clarified by centrifugation at 12,000 $\times g$ for 5 min and then resuspended in RIPA solution. The Promega CaspACE kit (Fluorometric Assay System Madison, Wisconsin, USA) was used to measure caspase activity. The clear lysates containing 50 μg of protein were incubated with either 50 μM Ac-DEVD-AMC (the substrate of caspase-3) or 50 μM Ac-YVAD-AMC (the substrate of caspase-1) at 30°C for 1 h. The levels of released AMC were monitored to measure caspase activity using a spectrofluorometer (Hitachi F-4500) with excitation at 360 nm and emission at 460 nm.

2.12. Immunoprecipitation and mitogen-activated protein (MAP) kinase activity assay

The cell extracts were centrifuged to remove cellular debris, and the protein content of supernatant was mea-

sured in the BCA protein assay. JNK-1, ERK-1, and p38 were immunoprecipitated and kinase activity was measured by using an immunokinase complex assay with the respective substrate, GST-c-Jun, GST-MBP, and GST-ATF2 as described (Kyriakis et al., 1994). Briefly, the cell lysates (200 μg of protein) were incubated with protein A-Sepharose and anti-JNK-1, anti-ERK-1, or anti-p38 (10 μg polyclonal antibody) overnight at 4°C. The immune complexes were pelleted and washed three times with cold PBS containing 1% Nonidet P-40 and 2 mM sodium orthovanadate, once with cold 100 mM Tris–HCl (pH 7.5) buffer containing 0.5 M LiCl, and once with cold kinase reaction buffer (12.5 mM morpholinepropanesulfonic acid [MOPS] [pH 7.5], 12.5 mM β-glycerophosphate, 7.5 mM $MgCl_2$, 0.5 mM EGTA, 0.5 mM NaF, 0.5 mM sodium orthovanadate). The kinase reaction was performed in the presence of 1 μCi of [γ-^{32}P] ATP, 20 μM of ATP, 3.3 μM of dithiothreitol, and 3 μg of substrates (GST-c-Jun-(1–35), GST-MBP, or GST-ATF2) in kinase reaction buffer at 30°C for 30 min. The samples were heated at 95°C for 5 min and resolved on 12% sodium dodecyl sulfate (SDS) gels. Phosphorylated substrates (GST-c-Jun, GST-MBP, or GST-ATF2) were visulaized by autoradiography. The kinase activity was expressed as fold of control.

2.13. Immunoblotting against JNK-1, ERK-1, p38, poly (ADP-ribose) polymerase, and Bcl-2

Equal amounts of lysate protein (50 μg/lane) were subjected to SDS-PAGE with 10% polyacrylamide gels and then electrophoretically transferred to nitrocellulose membrane. Nitrocellulose blots were first blocked with 3% bovine serum albumin in PBST buffer (PBS plus 0.01% Tween 20, pH 7.4) and then incubated overnight at 4°C with the primary antibody against JNK-1, ERK-1, p38, poly (ADP-ribose) polymerase, or Bcl-2 in PBST containing 1% bovine serum albumin. Immunoreactivity was detected by sequential incubation with horseradish peroxidase-conjugated secondary antibody, and detected by the enhanced chemiluminescence technique.

2.14. Statistic analysis of the data

Data are expressed as mean values ± standard error (S.E.M.). The statistical analysis was carried out with a one-way analysis of variance (ANOVA) followed by Dunnett's tests to assess the statistical significance ($P < 0.05$) between treated and untreated groups in all experiments.

3. Results

3.1. Effects of disulfiram–Cu^{2+} complex on the viability of rat cortical astrocytes

The cytotoxicity of disulfiram and Cu^{2+} either alone or in the complex form was examined in the MTT reduction assay. Our data showed that only high concentrations of either disulfiram or $CuCl_2$ could induce the death of rat cortical astrocytes; IC_{50} was 22 ± 1.6 μM and 180 ± 12.5 μM, respectively (Fig. 1A). Serum-free medium had no effect on disulfiram-induced cytotoxicity. Cu^{2+} alone at low concentrations of 0.1–10 μM was nontoxic. Cu^{2+} (10

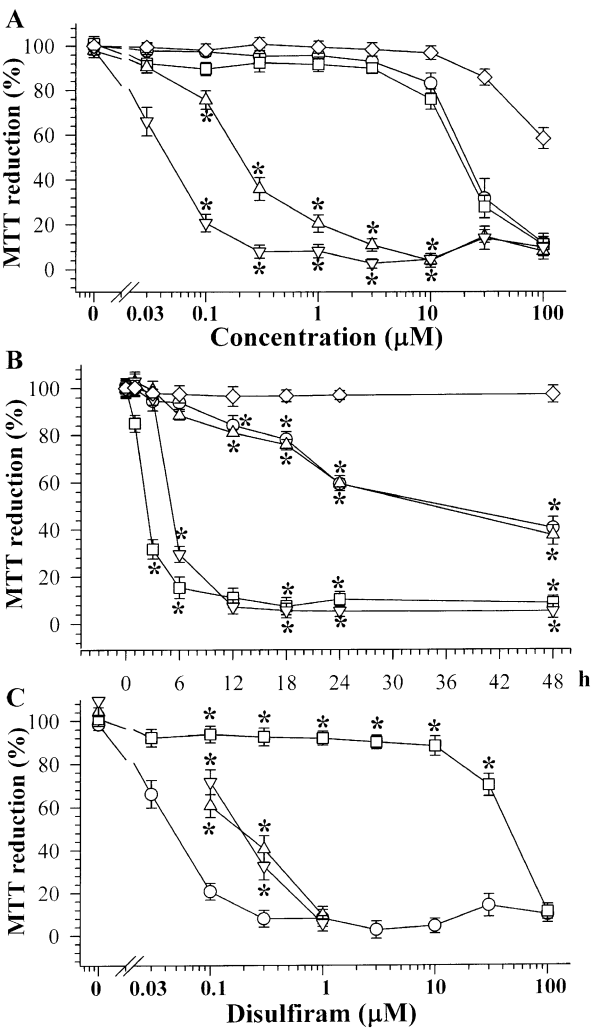

Fig. 1. Concentration- and time-dependent cytotoxicity induced by disulfiram–Cu^{2+} complex and its prevention by antioxidants and bath ocuproine disulfonate in rat cortical astrocytes. The viability of rat cortical astrocytes was determined by MIT assay after incubation with disulfiram plus various compounds at 37 ± 0.5°C for 24 h (A) or for various time intervals (B). Data are presented as means ± S.E. ($n = 6$). (A). Concentration-dependentcytoxicity of disulfiram without (○—○) or with $CuCl_2$ at 1 μM (□–□), 3 μM (△–△) and 10 μM (▽–▽) respectively. Cu^{2+} alone (◇–◇) also appeared to be cytotoxic. *: $P < 0.05$ as compared with that treated with disulfiram alone. (B). Time course of cytotoxicity induced by 300 μM $CuCl_2$ alone (○—○), 100 μM disulfiram alone (□–□), 0.1 μM disulfiram + 10 μM $CuCl_2$ (△–△) or 1 μM disulfiram + 10 μM $CuCl_2$ (▽–▽). *: $P < 0.05$ as compared with the vehicle control (◇–◇). (C). Prevention by 300 μM bathocuproine disulfonate (□–□), 3 mM vitamin C (▽–▽), or 3 nM NAC (△–△) of cytotoxicity induced by disulfiram + 10 μM $CuCl_2$ (○—○). *: $P < 0.05$ as compared to the control treated with disulfiram + 10 μM $CuCl_2$.

μM), but not $FeSO_4$, $FeCl_3$, Pb actate, and Pb nitrite, became very toxic in the presence of disulfiram (0.03–10 μM). $ZnCl_2$ had only a weak potentiating effect at concentrations of 10–100 μM. Fig. 1 shows that the disulfiram–Cu^{2+} complex had a cytotoxic effect in a concentration- and time-dependent manner. The IC_{50} of disulfiram was decreased by 10 μM $CuCl_2$, from 22 to 0.05 μM: the potentiation factor was 440-fold. Moreover, the disulfiram–Cu^{2+} complex induced cytotoxicity at a much faster rate than that induced by either 100 μM disulfiram or 300 μM $CuCl_2$ alone (Fig. 1B).

The antioxidant *N*-acetyl-cysteine (0.3–3 mM), but not GSH, could partially inhibit the cytotoxic effect of the complex (0.1–0.3 μM disulfiram–Cu^{2+}), but almost completely prevented that of 100 μM disulfiram alone. Vitamin C (0.3–3 mM), but not vitamin E (1–20 μM), could also partially reduce disulfiram–Cu^{2+} complex-induced toxicity (Fig. 1C). Bathocuproine disulfonate (100–300 μM) completely abolished the cytotoxicity induced by the complex but not that induced by 100 μM disulfiram. A higher concentration (20–25%) of fetal calf serum as well as bovine serum albumin (0.3–3%) significantly attenuated the cytotoxicity from $79 \pm 3.8\%$ to $54 \pm 4.9\%$ and $48 \pm 5.3\%$, respectively (Fig. 1C).

3.2. Disulfiram–Cu^{2+} complex caused DNA hypodiploidy

As shown in Fig. 2A and B, the disulfiram (0.3 μM)–Cu^{2+} (10 μM) complex caused DNA hypodiploidy in a time- and concentration-dependent manner. The amount of hypodiploid DNA was determined after staining with propidium iodide and then analyzed by flow cytometry. By contrast, neither 1 μM disulfiram nor 10 μM Cu^{2+} alone could induce hypodiploidy even after a 48-h incubation (Fig. 2B). This hypodiploid effect was apparently correlated with the cytotoxicity detected with the MTT assay. Bathocuproine disulfonate (Fig. 2B) and bovine serum albumin (1% and 3%) could abolish this hypodiploid characteristic by the disulfiram–Cu^{2+} complex.

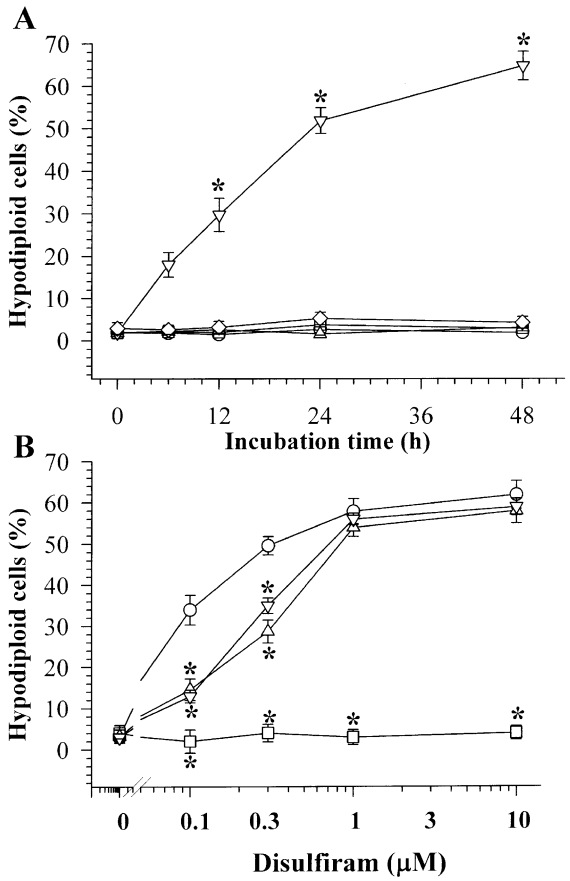

Fig. 2. Time course of hypodiploidy of DNA induced by disulfiram–Cu^{2+} complex and its prevention by bathocuproine disulfonate, *N*-acetyl-cysteine, and bovine serum albumin in rat cortical astrocytes. Astrocytes were treated with disulfiram–Cu^{2+} complex for various time intervals without (A) or with bathocuproine disulfonate, *N*-acetyl-cysteine, and vitamin C (B) for 24 h. DNA strands were analyzed after staining with propidium iodide coupled with flow cytometry. (A). Control, ○—○; disulfiram 0.3 μM, □–□; $CuCl_2$ 10 μM, △–△; disulfiram 0.3 μM + $CuCl_2$ 10 μM, ▽–▽ or disulfiram 0.3 μM + bathocuproine disulfonate 300 μM, ◇–◇. (B). Disulfiram + $CuCl_2$ 10 μM alone, ○—○; or with bathocuproine disulfonate 300 μM, □–□; *N*-acetyl-cysteine 3 mM, △–△; vitamin C, 3 mM, ▽–▽. Data are presented as means ± S.E. ($n = 3$). *: $P < 0.05$ compared with respective control.

3.3. Disulfiram–Cu^{2+} complex-induced morphological changes, and cell nuclei condensation

As shown in Fig. 3A (left panel), the normal control astrocytes (14DIV) were not only tightly attached to the culture plate but also to each other and formed a confluent layer of flat cells. By contrast, after treatment with the disulfiram–Cu^{2+} complex, the morphology of astrocytes changed dramatically, but not after treatment with bathocuproine disulfonate 300 μM, disulfiram 0.3 μM, or Cu^{2+} 10 μM alone. Astrocytes began to dissociate gradually within 1 h and then progressively became detached. Cell shrinkage, nuclear condensation and apoptic bodies became prominent after treatment for 6 h. After prolonged incubation for 12 h (data not shown), necrotic cells appeared and eventually extensive cell loss was found after 24 h (Fig. 3B and C). All of these morphological changes caused by the disulfiram–Cu^{2+} complex but not those caused by disulfiram 30–100 μM were completely prevented by the non-permeable specific Cu^{2+} chelator bathocuproine disulfonate (Fig. 3D), which suggests that the mechanisms of the toxic effects of disulfiram–Cu^{2+} complex and disulfiram may be different.

Staining the cell nuclei with the DNA-binding fluorochrome Höechst 33258, we showed that the disulfiram–Cu^{2+} complex, but not disulfiram 0.3 μM or Cu^{2+} 10 μM, induced nuclei condensation associated with apop-

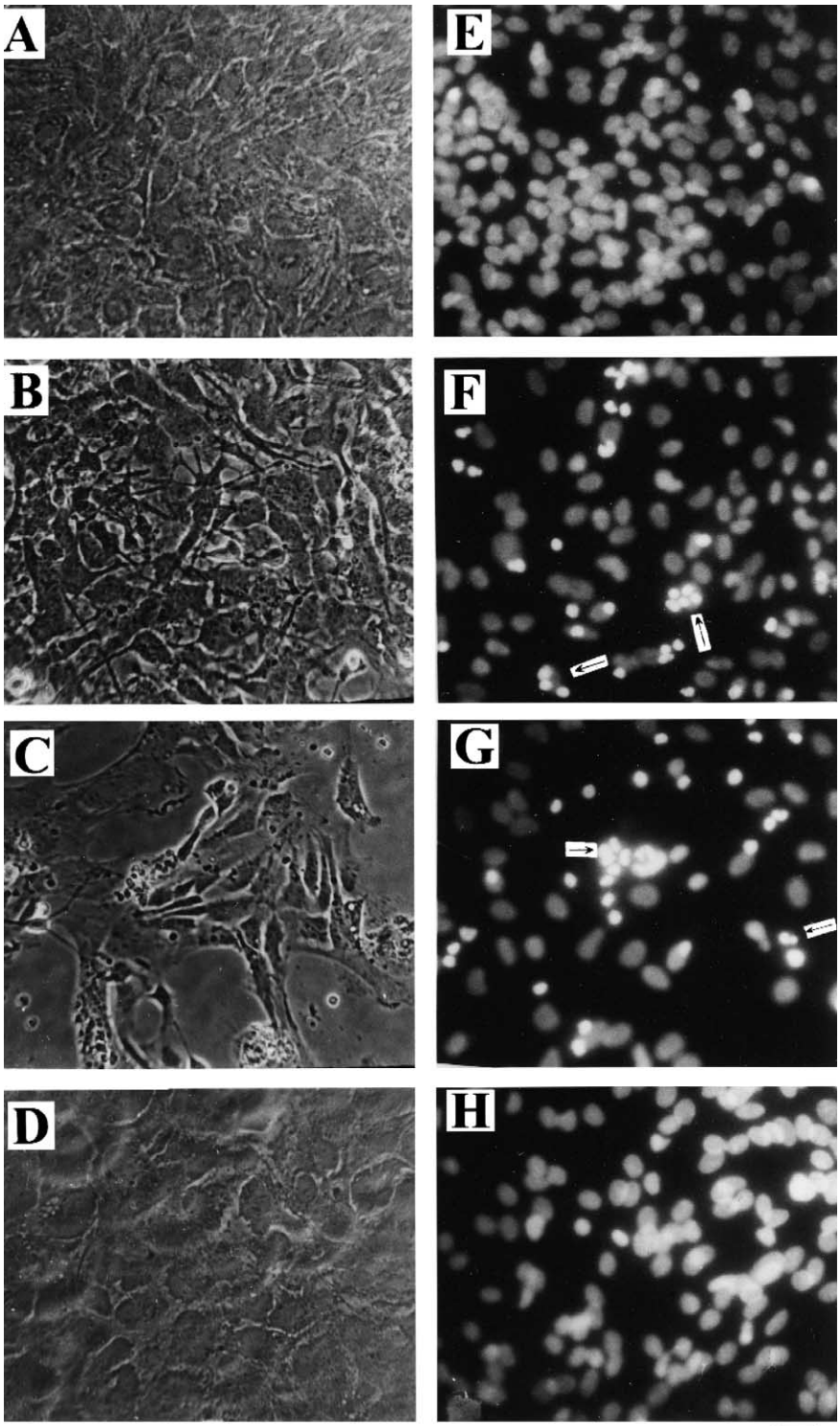

Fig. 3. Morphological changes induced by disulfiram–Cu^{2+} complex in cultured rat cortical astrocytes. Cells were treated without (A) or with the complex of disulfiram (0.3 μM) plus Cu^{2+} (10 μM) for either 6 h (B) or 24 h (C). Bathocuproine disulfonate 300 μM (D) prevented the morphological changes induced by disulfiram–Cu^{2+} complex in cells examined by phase-contrast microscopy (A). The apoptotic bodies were examined by flourescence-microscopy after fixation with 4% formaldehyde for 30 min at room temperature, and then stained with Hoechst dye 33258 (B). Arrows indicate apoptotic nuclei. Scale bar = 10 μM.

totic bodies (Fig. 3F and G, right panel). The nuclei of astrocytes became condensed and fragmented after a 3-h treatment with disulfiram (0.3 μM)–Cu^{2+} (10 μM) complex, and these effects appeared more severely at 6 h (Fig.

3F). Preincubation of astrocytes for 1 h with bathocuproine disulfonate (300 μM) abolished these detrimental effects of the disulfiram–Cu^{2+} complex (Fig. 3H).

3.4. Effects of disulfiram–Cu^{2+} complex on intracellular copper content

Neither a low (0.3 μM) nor a high (100 μM) concentration of disulfiram, nor Cu^{2+} (10 μM) alone significantly altered the total intracellular copper content (Fig. 4A). A higher concentration of 300 μM of Cu^{2+} alone and disulfiram (0.3 μM)–Cu^{2+} (10 μM) complex markedly increased the intracellular copper content after a 3-h incubation (Fig. 4A). The kinetics of the increase in copper content were similar in the subcellular fractions of the plasma membrane, cytosol, and nuclei (Fig. 4B). The copper content of the DNA fraction increased by 10-fold within 0.5 h and remained at a high level over a 0.5- to 48-h incubation (data not shown). The profile of the increase in copper content was closely correlated with the toxic effects revealed by the MTT reduction test, DNA

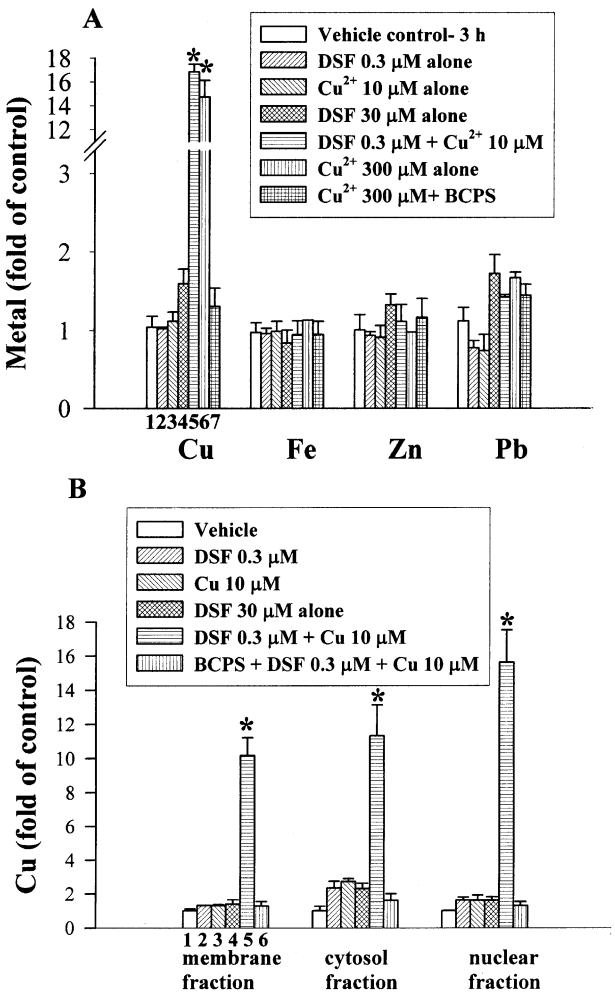

Fig. 4. Changes in cell trace metal content of rat cortical astrocytes after treatment with disulfiram–Cu^{2+} complex. Astrocytes were treated with disulfiram and Cu^{2+} either alone or complex 37 ± 0.5°C for 3 h, and then the cell trace metal content was assayed by inductively coupled plasma mass spectrometry (ICP-mass) (A). The Cu contents of the subcellar fractions were also assayed by atomic absorbance spectrophotometry (B) as described in Materials and methods. Data are expressed as fold of control, means ± S.E.M. The mean contents of Cu, Fe, Zn, and Pb of control cells were 14.36 ± 0.7, 251.32 ± 44.21, 126.05 ± 27.1, and 13.6 ± 1.9 ng/mg protein, respectively. The control Cu content of membrane fraction, cytosol, and nuclear fractions was 2.17 ± 0.35, 9.8 ± 1.8, and 1.25 ± 0.25 ng/mg protein, respectively.

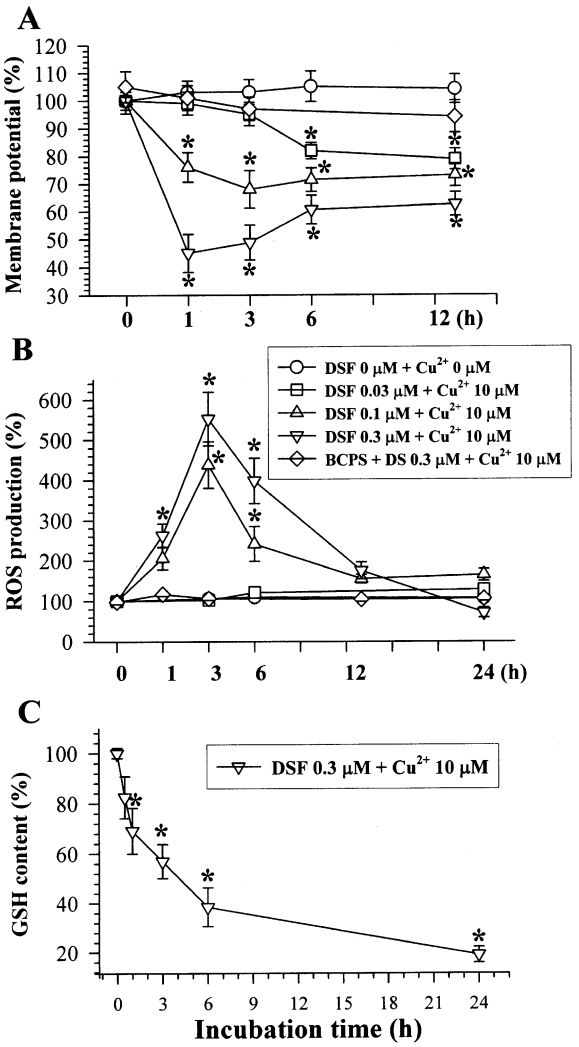

Fig. 5. Disulfiram–Cu^{2+} complex decreased the mitochondrial membrane potential and increased free radical production in rat cortical astrocytes. Cells were treated with disulfiram–Cu^{2+} complex for various times and then an aliquot of the cells was labeled with the fluorescent dye $DiOC_6$ (3) (A) or DCFHDA (B) for analyzing the fluorescence intensity with flow cytometry as described in Materials and methods. The astrocytes were incubated for different times and then the reduced glutathione (GSH) content of cell extracts was determined with a colorimetric method and compared with GSH standard (C). Data are presented as means ± S.E. ($N = 3$). *: $P < 0.05$ as compared with respective control.

hypodiploidy, and the morphological changes. The non-permeable specific copper chelator bathocuproine disulfonate 300 μM prevented all these effects of the disulfiram (0.1–10 μM)–Cu^{2+} (3–10 μM) complex (Figs. 1C, 2B, and 3D,H). These findings indicate that the disulfiram–Cu^{2+} complex entered the cells and dramatically increased the copper content of the cytosolic and nuclear fractions. Since both H_2O_2 production and GSH reduction occurred before the morphological changes and cytotoxicity, we propose that the cytotoxic effect of the disulfiram–Cu^{2+} complex is probably mediated by free radical production and non-protein thiol depletion.

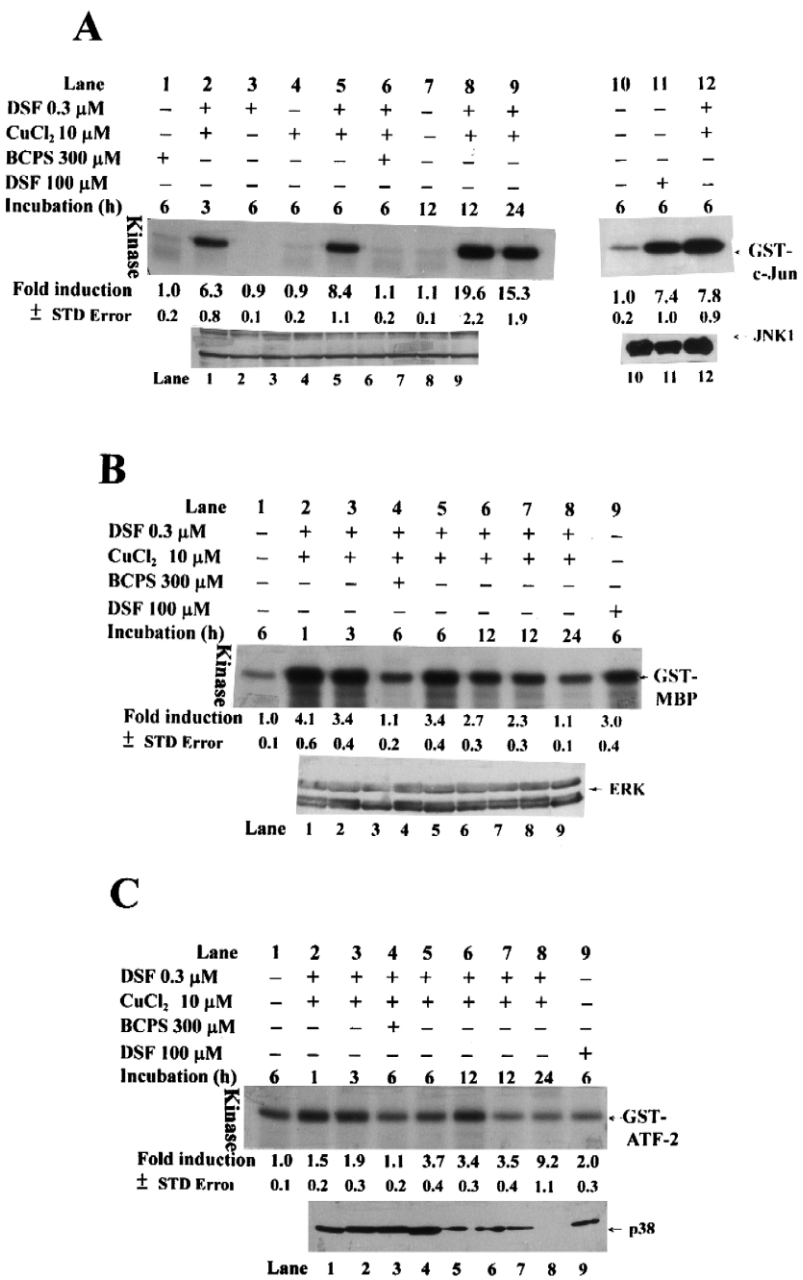

Fig. 6. Bathocuprione disulfonate abolished the time-dependent activation of mitogenactivated protein kinase induced by disulfiram–Cu^{2+} complex in rat cortical astrocytes. Astrocytes were treated with disulfiram–Cu^{2+} complex for various intervals. The cell lysates were prepared and immunoprecipitated with 10 μg of polyclonal anti-JNKl antibody (A), anti-ERK-1 antibody (B) or anti-p38 antibody (C), followed by 20 μl of Sepharose A-conjugated protein A. The kinase reaction was performed as described in Materials and methods. The top figure represents the autoradiogram of [γ^{32}P] ATP incorporation into exogenous GST-c-Jun (1-135) (A), GST-MBP (B) or GST-ATF-2 (C). The amount of cell lysates used was 200 μg of protein in each lane. The bottom figure shows Western blots performed with antibody specific to anti-JNK-1 antibody (A), anti-ERK-1 antibody (B), or anti-p38 antibody (C). The fold induction in this figure is presented as the ratio of JNK activity to JNK-1 protein, ERK activity to ERK-1 protein, p38 activity to p38 protein against time. The values in this figure are presented as means of three determinations.

3.5. Disulfiram–Cu^{2+} complex decreased mitochondrial membrane potential, increased free radical production and reduced non-protein thiols content

We monitored the effects of the disulfiram–Cu^{2+} complex on the mitochondrial transmembrane potential ($\Delta\psi_m$) by using fluorescent probe $DiOC_6(3)$ coupled with flow cytometric analysis. Treatment of astrocytes with disulfiram–Cu^{2+} complex produced a significant, steady decline in $DiOC_6(3)$ accumulation, indicating the loss of the mitochondrial membrane potential (Fig. 5). The onset of the decrease in mitochondrial membrane potential was dependent on the disulfiram concentration (0.03–0.3 μM, Fig. 5A). Bathocuproine disulfonate also abolished this effect of the disulfiram–Cu^{2+} complex. By means of fluorochrome DCFHDA coupled with a flow cytometric technique, we showed that the disulfiram Cu^{2+} complex increased free radical production in a concentration- and time-dependant manner (Fig. 5B). This effect was already visible after 1 h and reached a peak at 3 h. We also found that disulfiram (0.3 μM)$^{2+}$ (10 μM) complex rapidly decreased the GSH content to 68 ± 5.7% of control within 1 h and to 22 ± 1.9% at 24 h (Fig. 5C).

3.6. Activation of the JNK, ERK, and p38 kinase activity

We examined the effects of disulfiram 100 μM alone or disulfiram–Cu^{2+} complex on JNK activity by detecting the phosphorylation of its substrate c-Jun and JNK protein expression. As shown in Fig. 6A, disulfiram–Cu^{2+} complex markedly increased JNK activity by sixfold after a 3-h incubation, reaching a plateau at 12 h (an increase of about 19-fold), an effect which was sustained until 24 h. Disulfiram 0.3 μM, Cu^{2+} 10 μM, and bathocuproine disulfonate 300 μM alone did not increase JNK activity, but a higher concentration of 100 μM disulfiram significantly increased JNK activity (Fig. 6A) but to a lesser extent, by about sevenfold at 6 h. However, JNK-1 protein remained unaltered after treatment with disulfiram–Cu^{2+} complex. The activation of JNK could be prevented by the specific Cu^{2+} chelator-bathocuproine disulfonate at both 6 h (Fig. 6A) and the other times tested (data not shown). By contrast, disulfiram 100 μM and disulfiram–Cu^{2+} complex only transiently induced ERK activation, as detected by phosphorylation of its substrate myelin basic protein (MBP), as early as 1 h about fourfold, and ERK activity gradually decreased to a basal level at 24 h (Fig. 6B). Bathocuproine disulfonate also blocked this activation. ERK-1 protein expression did not significantly change. It appeared that p38 kinase was not activated early at 1 to 3 h and that the p38 protein was not degraded. However, 6 h after the addition of disulfiram 100 μM and 24 h after incubation with the disulfiram–Cu^{2+} complex (Fig. 6C), the activation of p38 accompanied by degradation of p38 protein was found. For the control studies, we found that bathocuproine disulfonate 300 μM, disulfiram 0.3 μM and Cu^{2+} 10 μM alone did not activate the ERK and p38 kinases (data not shown) nor JNK (Fig. 6A).

3.7. Disulfiram–Cu^{2+} complex stimulated caspase-3 activity and poly (ADP-ribose) polymerase degradation in a time-dependent manner

We used a fluorogenic peptide substrate (Ac-DEVD-AMC) as a specific substrate for caspase-3. Caspase activity was monitored following treatment of astrocytes with disulfiram–Cu^{2+} complex for various times. As shown in Fig. 7A, disulfiram–Cu^{2+} complex caused an increase in caspase-3 activity in astrocytes with an onset at 6 h and a maximum at 12 h. This level of activity persisted until 36 h after treatment. Bathocuproine disulfonate also abolished

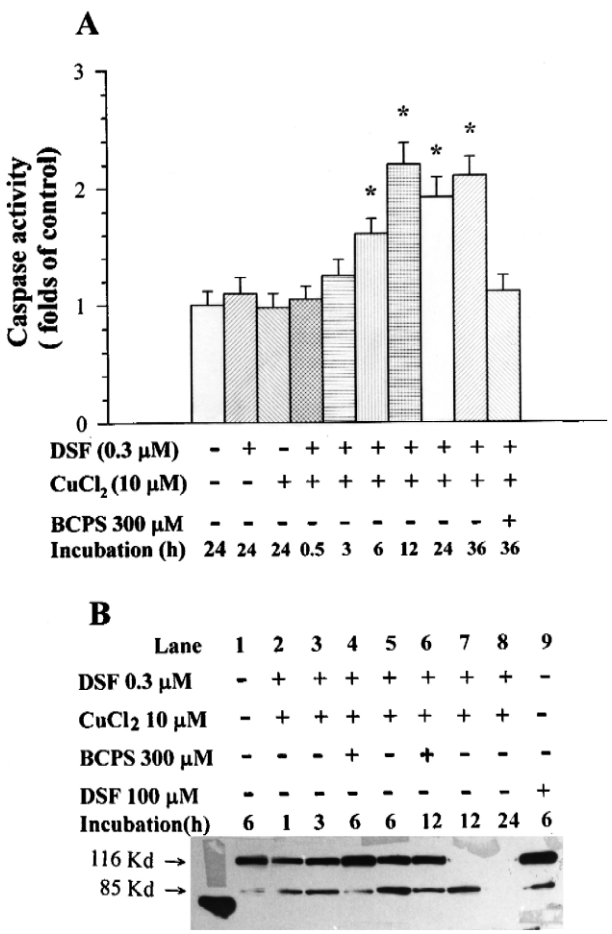

Fig. 7. BCPS blocked the caspase activation and cleavage of PARP from 116 kDa to 85 kDa induced by the disulfiram–Cu^{2+} complex in time-dependent manner in rat cortical astrocytes (A). Cells were treated with disulfiram 0.3 μM and Cu^{2+} 10 μM complex for various intervals as indicated, and then caspase activity was measured as described in Materials and methods. (B) The Western blots were performed with antibody specific to anti-poly (ADP-ribose) polymerase antibody. The amount of cell lysates used was 50 μg of protein in each lane. This panel is a plot of the ratio of 85 to 116 kDa protein against time. The values in this figure are presented as means and standard errors of three determinations. *: $P < 0.05$ compared with respective control.

this activation of caspase-3 by disulfiram–Cu^{2+} complex (Fig. 7A).

We further examined whether the endogenous poly (ADP-ribosyl) polymerase 116-kDa protein (one of caspase substrate) was cleaved to generate a 85-kDa fragment. As shown in Fig. 7B, disulfiram–Cu^{2+} complex caused the degradation of 116-kDa poly (ADP-ribosyl) polymerase into an 85-kDa fragment in a time-dependent manner. We also found that bathocuproine disulfonate effectively inhibited the cleavage of poly (ADP-ribosyl) polymerase induced by disulfiram–Cu^{2+} complex (Fig. 7B). For a negative control experiment, the Bcl-2 protein was detected by Bcl-2 antibody and was found to have non-significantly changed after treatment with disulfiram–Cu^{2+} complex (data not shown).

4. Discussion

In this study, we attempted to elucidate the mechanisms of the cytotoxic effects induced by either disulfiram, Cu^{2+} alone or by disulfiram–Cu^{2+} complex in primary cultures of rat astrocytes. The results obtained suggested that disulfiram–Cu^{2+} complex initially caused an increase in intracellular Cu content followed by a reduction of mitochondrial membrane potential, free radical generation and GSH depletion. The subsequent activation of JNK, caspase-3 and poly (ADP-ribosyl) polymerase degradation is believed to be responsible for triggering the apoptotic process induced by the disulfiram–Cu^{2+} complex in the cultured astrocytes.

In our preliminary test, we examined the cytotoxic effect of the combination of disulfiram and various metal salts. The results obtained showed that Cu^{2+}, but not other metal ions (3–10 μM of Pb^{2+}, Zn^{2+}, Fe^{3+}), could markedly potentiate the toxicity of disulfiram. It was therefore considered that disulfiram is a more selective chelator of Cu^{2+} than of other metal ions under our experimental conditions in rat cortical astrocytes. This finding is different from that found in the brain, where disulfiram potentiates the effect of lead in inducing neuronal depression (Oskarsson et al., 1986). Luthman et al. (1991) have also shown that disulfiram alters the expression of glial fibrillary acidic protein in astrocytes.

Cu^{2+} is an essential metal ion in animals. Serum normally contains 0.3–0.6 ppm of copper in mice (Massie et al., 1993) and 1 ppm (16 μM) in humans (Graham et al., 1991). Therefore, in the present work, we studied the potentiating effect of Cu^{2+} at a low concentration (10 μM) on disulfiram-induced cytotoxicity in astrocytes. The results obtained may provide crucial information for understanding the molecular mechanism of the cytotoxic effects of disulfiram in a low Cu^{2+} environment. Disulfiram (0.1–10 μM) combined with a fixed concentration (10 μM, 0.6 ppm) of Cu^{2+} induced apoptosis in astrocytes in a concentration- and time-dependent manner. Actinomycin D could not block the cytotoxicity induced by disulfiram alone or that induced by the disulfiram–Cu^{2+} complex. It is thus suggested that RNA synthesis may not be involved in this toxic mechanism. The appearance of hypodiploid DNA, nuclear condensation and apoptotic bodies suggests that the cell death induced by the disulfiram–Cu^{2+} complex may be mediated by apoptosis. The toxicity of disulfiram alone and that of the disulfiram–Cu^{2+} complex in calcium free- or 20 mM Ca^{2+}-DMEM was not significantly different from the toxicity seen in normal DMEM containing 2 mM Ca^{2+}. This finding is in agreement with that found in hepatocytes (Dogterom and Mulder, 1993), namely, that external Ca^{2+} is not essential for the cytotoxic effect of the disulfiram–Cu^{2+} complex.

Mitochondrial dysfunction has been proposed to play a critical role in inducing apoptosis (Nieminen et al., 1995; Vavssiäre et al., 1994). Mitochondrial membrane depolarization as a result of opening of the permeability transition pores is an early irreversible event during apoptosis (Zamzami et al., 1995). Moreover, the generation of free radicals in mitochondria may result in mitochondrial lipid peroxidation (Bruce-Keller et al., 1998). In our studies, disulfiram–Cu^{2+} complex significantly decreased the mitochondrial membrane potential ($\Delta\psi_m$), followed by an increase in reactive oxygen species generation and in glutathione depletion (Fig. 5). Since the Cu^{2+}-chelator bathocuproine disulfonate, and the antioxidants *N*-acetylcysteine and vitamin C could inhibit the cytotoxic effects of the disulfiram–Cu^{2+} complex, it is proposed that the disulfiram–Cu^{2+} complex induced apoptosis mediated by an increase in the Cu content and in oxidative stress. The method we used to determine the total Cu content did not distinguish between protein bound and unbound Cu. Whether the intracellular Cu^{2+} and/or bound Cu is responsible for this death signaling is not clear and needs further investigation.

The MAP kinase family, which includes JNK, extracellular signal regulated kinase (ERK), and p38 kinase, can be rapidly activated by various stressors (Robinson and Cobb, 1997). Recent evidence suggests that the stress-activated protein kinase (SAPK)/JNK pathway may play an important role in triggering apoptosis in response to seramide (Verheij et al., 1996), inflammatory cytokines (Chen et al., 1996; Zhang et al., 1996), free radicals generated by UV-C, gamma radiation (Hibi et al., 1993; Alder et al., 1995), direct application of hydrogen peroxide (Yu et al., 1996), DNA-damaging agents (Kharbanda et al., 1995; Potapova et al., 1997) and alkylating agents (Derijard et al., 1994). The downstream signaling pathway of activated JNK could be cascape-3 (Takahashi et al., 1999; Harada and Sugimoto, 1999). A number of cascape-3 protease targets have been identified, including the nuclear enzyme poly (ADP-ribose) polymerase, which can be activated by staurosporine, leading to apoptosis in astrocytes (Keane et al., 1997). Our findings obtained also suggested that disulfiram and disulfiram–Cu^{2+} complex induced the

apoptotic process through the signaling pathway of oxidative stress-JNK-cascape 3-poly (ADP-ribose) polymerase degradation. A different activation of JNK, ERK, and p38 by disulfiram–Cu^{2+} complex was found. The sustained activation of JNK for more than 24 h (Fig. 6) contrasted with the transient activation of ERK and p38. The subsequent activation of cascape-3 and then the degradation of poly (ADP-ribose) polymerase are believed to be involved in the process of apoptosis (Fig. 7). All of these cellular events induced by the disulfiram–Cu^{2+} complex were Cu^{2+} dependent, since the intracellular Cu content was markedly increased and the chelation of extracellular Cu^{2+} with bathocuproine disulfonate prevented not only the activation of these cellular events but also cell death, confirming the early mediating role of Cu^{2+} during disulfiram–Cu^{2+} complex-induced cell death. Since the glutathione precursor *N*-acetyl-cysteine could block both the cytotoxic effect and MAP kinase activation induced by the disulfiram–Cu^{2+} complex, it is reasonable to infer that the radical signal is primary and essential to the initiation of the JNK signaling cascade, as suggested by Xia et al. (1995).

In conclusion, our results indicate that a low concentration of (0.03–10 μM) disulfiram combined with a low concentration (10 μM) of Cu^{2+} potently induces apoptosis in cultured rat cortical astrocytes. The underlying molecular mechanisms were explored. We found that an increased intracellular Cu content was essential for the cellular events induced by disulfiram–Cu^{2+} complex, including a decrease in the mitochondrial membrane potential, an increase in free radical production and depletion of the GSH content. The downstream signaling pathway was shown to involve the activation of JNK and caspase-3 followed by poly (ADP-ribose) polymerase degradation. The implication of this study is that the chronic toxicity of disulfiram, such as axonal degeneration and neurotoxicity, in patients may be, at least in part, due to the formation of the pro-oxidant complex of disulfiram and Cu^{2+} in vivo.

Acknowledgements

This investigation was supported by the National Science Council (NSC 87-2314-B-002-085), Taipei, Taiwan.

References

Alder, V., Schaffer, A., Kim, J., Dolan, L., Ronai, Z., 1995. UV irradiation and heat shock mediate JNK activation via alternate pathways. J. Biol. Chem., 270, 26071–26077.

Amruthesh, S.C., Boerschel, M.F., McKinney, J.S., Willoughby, K.A., Ellis, E.F., 1993. Metabolism of arachidonic acid to epoxyeicosatrienoic acids, hydroxyeicosatetraenoic acids and prostaglandin's in cultured rat hippocampal astrocytes. J. Neurochem., 61, 150–159.

Ansbacher, L.E., Bosch, E.P., Cancilla, P.A., 1982. Disulfiram neuropathy: a neurofilamentous distal axonpathy. Neurology, 32, 424–428.

Bezuglyi, V.P., Ivanova, S.I., Il'ina, V.I., Komarova, L.I., Fokina, K.V., 1982. Health status of persons working with copper-containing and other pesticides. Vrach. Delo, 1, 107–109.

Brown, D.R., 1999. Neurons depend on astrocytes in a coculture system for protection from glutamate toxicity. Mol. Cell. Neurosci., 13, 379–389.

Bruce-Keller, A.J., Begley, J.G., Fu, W., Butterfield, D.A., Bredesen, D.E., Hutchins, J.B., Hensley, K., Mattson, M.P., 1998. Bcl-2 protects isolated plasma and mitochondrial membranes against lipid peroxidation induced by hydrogen peroxide and amyloid beta-peptide. J. Neurochem., 70, 31–39.

Chen, F., Sun, S.C., Kuh, D.C., Gaydos, L.J., Demers, L.M., 1995. Essential role of NF-kappa B activation in silica-induced inflammatory mediator production in macrophages. Biochem. Biophys. Res. Commun., 214, 985–992.

Chen, Y.-R., Wang, X., Templeton, D., Davis, R., Tan, T.-H., 1996. The role of c-Jun N-terminal kinase (JNK) in apoptosis induced by ultraviolet C and radiation. J. Biol. Chem., 271, 31929–31936.

Delmaestro, E., Trombetta, L.D., 1995. The effects of disulfiram on the hippocampus and cerebellum of the rat brain: a study on oxidative stress. Toxicol. Lett., 75, 235–243.

Denizot, F., Lang, R., 1986. Rapid colorimetric assay for cell growth and survival. Modification to the tetrazolium dye procedure giving improved sensitivity and reliability. J. Immunol. Methods, 89, 271–277.

Derijard, B., Hibil, M., Wu, L.-H., Barret, T., Su, B., Deng, T., Karin, M., Davis, R., 1994. JNK1: a protein kinase stimulated by UV light and Ha-Ras that binds and phosphorylates the c-Jun activation domain. Cell, 76, 1025–1037.

Dogterom, P., Mulder, G.J., 1993. Differential effects of extracellular calcium on lipid peroxidation dependent (ethacrynic acid and allyl alcohol) and lipid peroxidation independent (disulfiram)-induced cytotoxicity in normal and vitamin E-deficient rat hepatocytes. Chem.-Biol. Interact., 86, 171–181.

Friel, J.K., Skinner, C.S., Jackson, S.E., Longerich, H.P., 1990. Analysis of biological reference materials, prepared by microwave dissolution, using inductively coupled plasma mass spectrometry. Analyst, 115, 269–273.

Goedde, H.W., Agarwal, D.P., 1992. Pharmacogenetics of aldehyde dehydrogenase. In: Kalow, W. (Ed.), Pharmacogenetics of Drug Metabolism. Pergamon, New York, pp. 281–311.

Graham, N.M., Sorensen, D., Odaka, N., Brookmeyer, R., Chan, D., Willet, W.C., Morris, J.S., Saah, A.J., 1991. Relationship of serum copper and zinc level to HIV-1 seropositivity and progression to AIDS. J. AIDS, 4, 976–980.

Griffith, O.W., 1980. Automated test systems for the determination of deoxy sugars and 3-deoxy-D-arabinoheptulosonate-7-phosphate synthase. Anal. Biochem., 106, 207–212.

Harada, J., Sugimoto, M., 1999. An inhibitor of p38 and JNK MAP kinases prevents activation of caspase and apoptosis of cultured cerebellar granule neurons. Jpn. J. Pharmacol., 79, 369–378.

Hibi, M., Lin, A., Smeal, T., Minden, A., Karin, M., 1993. Identification of an oncoprotein- and UV-responsive protein kinase that binds and potentiates the c-Jun activation domain. Genes Dev., 7, 2135–2148.

Johansson, B., 1992. A review of the pharmacokinetics and pharmacodynamics of disulfiram and its metabolites. Acta Psychiatr. Scand., 86, 15–26.

Keane, R.W., Srinivasan, A., Foster, L.M., Testa, M.P., Ord, T., Nonner, D., Wang, H.G., Reed, J.C., Bredesen, D.E., Kayalar, C., 1997. Rapid communication activation of CPP32 during apoptosis of neurons and astrocytes. J. Neurosci. Res., 48, 168–180.

Kennedy, T., Ghio, A.J., Reed, W., Samer, J., Zagorski, J., Quay, J., Carter, J., Dailey, L., Hoidal, J.R., Devlin, R.B., 1998. Copper-dependent inflammation and nuclear factor-kappaB activation by particulate air pollution. Am. J. Respir. Cell Mol. Biol., 19, 366–378.

Kharbanda, S., Ren, R., Pandey, P., Shafman, T.D., Feller, S.M., Weichselbaum, R.R., Kufe, D.W., 1995. Activation of the c-Abl-tyrosine kinase in the stress response to DNA-damaging agents. Nature, 376, 785–788.

Kostova, V., 1995. The neurological screening of workers in the manufacture of copper and aluminum rolled wire. Probl. Khig., 20, 198–209.

Kuffler, S.W., Nicholls, J.G., Martin, A.R., 1984. From Neuron to Brain. Sinauer Associates, Sunderland, MA, pp. 323–360.

Kyriakis, J., Banerjee, P., Nikolakaki, E., 1994. The stress-activated protein kinase subfamily of c-Jun kinases. Nature, 369, 156–160.

Langeveld, C.H., Jongenelen, C.A., Schepens, E., Stoof, J.C., Bast, A., Drukarch, B., 1995. Cultured rat striatal and cortical astrocytes protect mesencephalic dopaminergic neurons against hydrogen peroxide toxicity independent of their effect on neuronal development. Neurosci. Lett., 192, 13–16.

Luthman, J., Olson, L., Bjorklund, H., Henschen, A., Hoffer, B., Oskarsson, A., 1991. Combined lead acetate and disulfiram treatment-induced alterations of glial fibrillary acidic protein (GFA) immunoreactive astrocytes in brain smears. Toxicology, 65, 333–346.

Madrigal-Bujaidar, E., Velazquez-Guadarrama, N., Morales-Ramirez, P., Mendiola, M.T., Martinez, A.L., Chamorro, G., 1999. Sister-chromatin exchanges induced by disulfiram in bone marrow and spermatogonial cells of mice treated in vivo. Food Chem. Toxicol., 37, 757–763.

Massie, H.R., Ofosu-Appiah, W., Aiello, V.R., 1993. Elevated serum copper is associated with reduced immune response in aging mice. Gerontology, 39, 136–145.

Nieminen, A.L., Saylor, A.K., Tesfai, S.A., Herman, B., Lemasters, J.J., 1995. Contribution of the mitochondrial permeability transition to lethal injury after exposure of hepatocytes to *t*-butylhydroperoxide. Biochem. J., 307, 99–106.

Oskarsson, A., Olson, L., Palmer, M.R., Lind, B., Björklund, H., Hoffer, B., 1986. Increased lead concentration in brain and potentiation of lead-induced neuronal depression in rats after combined treatment with lead and disulfiram. Environ. Res., 41, 623–632.

Pastorino, J.G., Chen, S.-T., Tafani, M., Snyder, J.-W., Farber, J.-F., 1998. The overexpression of Bax produces cell death upon induction of the mitochondria permeability transition. J. Biol. Chem., 273, 7770–7775.

Potapova, O., Haghighi, A., Bost, F., Liu, C., Birrer, M.J., Gjerset, R., Mercola, D., 1997. The Jun kinase/stress-activated protein kinase pathway functions to regulate DNA repair and inhibition of the pathway sensitizes tumor cells to cisplatiton. J. Biol. Chem., 272, 14041–14044.

Robinson, M.J., Cobb, M.H., 1997. Mitogen-activated protein kinase pathways. Cell Biol., 9, 180–186.

Rosenkranz, A.R., Schmaldienst, S., Stuhlmeier, K.M., Chen, W., Knapp, W., Zlabinger, G.J., 1992. A microplate assay for the detection of oxidative products using 2′,7′-dichlorofluorescin-diacetate. J. Immunol. Methods, 156, 39–45.

Rothstein, J.D., Dykes-Hoberg, M., Corson, L.B., Becker, M., Cleveland, D.W., Price, D.L., Wong, P.C., 1999. The copper chaperone CCS is abundant in neurons and astrocytes in human and rodent brain. J. Neurochem., 72, 422–429.

Simonian, J., Halder, D., Delmaestro, E., Trombetta, L.D., 1992. Effect of disulfiram (DS) on mitochondria from rat hippocampus: metabolic compartmentation of DS neurotoxicity. Neurochem. Res., 17, 1029–1035.

Takahashi, K., Inanami, O., Kuwabara, M., 1999. Effects of intracellular calcium chelator BAPTA-AM on radiation-induced apoptosis regulated by activation of SAPK/JNK and caspase-3 in MOLT-4 cells. Int. J. Radiat. Biol., 75, 1099–1105.

Talbot, V., 1986. Seasonal variation of copper and zinc concentrations in the oyster *saccostrea cucullata* from the damper archipelago, Western Australia: implications for pollution monitoring. Sci. Total Environ., 57, 217–230.

Tedeschi, B., Barreett, J.N., Keane, R.W., 1986. Astrocytes produce interferon that enhances the expression of H-2 antigens on a subpopulation of brain cells. J. Cell. Biol., 102, 2244–2253.

Vaccari, A., Saba, P.L., Ruiu, S., Collu, M., Devoto, P., 1996. Disulfiram and diethyldithiocarbamate intoxication affects the storage and release of striatal dopamine. Toxicol. Appl. Pharmacol., 139, 102–108.

Vavssiäre, J.-L., Petit, P.X., Risler, Y., Mignotte, B., 1994. Commitment to apoptosis is associated with changes in mitochondrial biogenesis and activity in cell lines conditionally immortalized with simsan virus 40. Proc. Natl. Acad. Sci. U. S. A., 91, 11752–11756.

Verheij, M., Bose, R., Lin, X., Yao, B., Jarvis, W., Grant, S., Birrer, M., Szabo, E., Zon, L., Kyriakis, J., Haimovitz-Friedman, A., Fuks, Z., Kolesnick, R., 1996. Requirement for ceramide-initiated SAPK/JNK signaling in stress-induced apoptosis. Nature, 380, 75–79.

Xia, Z., Dickens, M., Raingeaud, J., Davis, R.J., Greenberg, M.E., 1995. Opposing effects of ERK and JNK-p38 MAP kinases on apoptosis. Science, 270, 1326–1331.

Yu, R., Jiao, J.J., Duh, J.L., Tan, T.H., Kong, A.H., 1996. Phenethyl isothiocyanate, a natural chemopreventive agent, activates c-Jun N-terminal kinase 1. Cancer Res., 56, 2954–2959.

Zamzami, N., Marchetti, P., Castedo, M., Decaudin, D., Macho, A., Hirsch, T., Susin, S.A., Petit, P.X., Mignotte, B., Kroemer, G., 1995. Sequential reduction of mitochondrial transmembrane potential and generation of reactive oxygen species in early programmed cell death. J. Exp. Med., 182, 367–377.

Zhang, Y.Y., Lind, B., Radmark, O., Samuelsson, B., 1993. Iron content of human 5-lipoxygenase, effects of mutations regarding conserved histidine residues. J. Biol. Chem., 268, 2535–2541.

Zhang, P., Miller, B.S., Rosenzweig, S.A., Bhat, N.R., 1996. Activation of c-Jun N-terminal kinase/stress-activated protein kinase in primary glial cultures. J. Neurosci. Res., 46, 114–121.